

A Technical Note on Atomic Beam Fluorescence Measurements for the Design of a Single Atom Microscope

Kristen Parzuchowski

June 22, 2017

Abstract

The Single Atom Microscope (SAM) will be used to measure rare nuclear reaction rates relevant for nuclear astrophysics. SAM will capture and detect all of the product atoms of the reactions of interest inside of a solid film of Neon. A detailed understanding of the number of atoms embedded in Neon is necessary in order to determine the intrinsic brightness of the product atoms in medium. This technical note describes the current status of the atom number in medium calibration including all assumptions made.

1 Introduction

The Single Atom Microscope is a new detector we are designing in order to measure rare nuclear reactions relevant for Nuclear Astrophysics. This detector captures and detects all product atoms of the reaction of interest inside of solid Neon. Our detection is highly efficient, because the solid Neon will capture all product, highly selective, because the product atoms are selected using resonant laser excitation, and highly sensitive, because there is a large shift between the emission and excitation spectrum of the product atom which significantly suppresses scattered light background from the laser [1,2]. My primary interest is in determining exactly how sensitive our technique is, or what the intrinsic brightness of our product atoms in solid Neon is. A low intrinsic brightness will require long integration times in order to detect single atoms.

A number of things must be known in order to determine the intrinsic brightness of the product atoms in medium:

- **Number density of atoms embedded in medium**
- Illumination laser intensity and beam profile
- Light collection efficiency
- Background sources present

This technical note focuses on calibrating the number density of atoms embedded in medium. To do this I perform atomic beam fluorescence measurements and simulations.

2 Atomic Structure of Yb

Ytterbium is a metallic chemical element in the lanthanide series. The valence shell of yb contains two electrons ($[\text{Xe}]4f^{14}6s^2$).

2.1 Isotopic Abundance

The ytterbium in our studies is in natural isotopic abundance, given in the table below.

Isotope	Abundance	Nuclear Spin, I
168	0.126 %	0
170	3.023%	0
171	14.216%	1/2
172	21.754%	0
173	16.098%	5/2
174	31.896%	0
168	12.887%	0

2.2 Hyperfine Structure

The hyperfine structure of an atom is a result of the interaction of the nucleon spin with the electron spin. For a given total electron angular momentum, J , and a total nuclear spin angular momentum, I , a total angular momentum can be calculated:

$$\vec{F} = \vec{J} + \vec{I} \quad (1)$$

For Yb, $J = 1$. Only isotopes with nonzero nuclear spin will be split into a hyperfine structure of states. For ^{171}Yb , $F = 1/2, 3/2$ and for ^{173}Yb , $F = 3/2, 5/2, 7/2$.

2.3 Frequency Splittings

The frequency splittings of Yb have been studied and measured a number of times before, so these values can be found in published papers. In the table below, the values I gathered from [3] are listed.

Isotope	Shift from ^{174}Yb (MHz)
176	-509.310(50)
173 (F=5/2)	-253.418(50)
173 (F=3/2)	515.975(200)
172	533.309(53)
173 (F=7/2)	587.986(56)
171 (F=3/2)	832.436(50)
171 (F=1/2)	1153.696(61)
170	1192.393(66)
168	1887.400(50)

3 Apparatus

The apparatus used for these studies is the setup for the Single Atom Microscope.

3.1 Atomic Oven

The atomic oven is the source of Yb for our atomic beam. This oven is rated for 450°C, which at this operating temperature will well satisfy our requirements for Yb number density in vacuum. From theory [2] of effusive beam sources, atomic beam flux has the relation: $Flux \propto \frac{P}{\sqrt{m}}$, where P is the vapor pressure of the atoms and m is the mass of atom. The vapor pressure of Yb and Mg at various temperatures is shown in figure 1. As Mg has a smaller mass and a larger vapor pressure than Yb, we can expect that this atomic oven will also satisfy the number density requirements for Mg.

The oven design and dimensions are shown in figure 2. The atomic beam effuses through a long circular cylindrical tube aperture on the oven. If l , the length of the cylindrical tube, is much larger than, r , the radius of the aperture, the number of atoms emerging from the source per unit time can be predicted theoretically by[2]:

$$Q = \frac{2}{3} \frac{r}{l} n \bar{v} A, \quad (2)$$

where n is the number of atoms per unit volume, \bar{v} is the mean atomic velocity and A is the area of the source slit. In our case, $l = 0.500''$ and $r = 0.0625''$, so our assumption is satisfied fairly well.

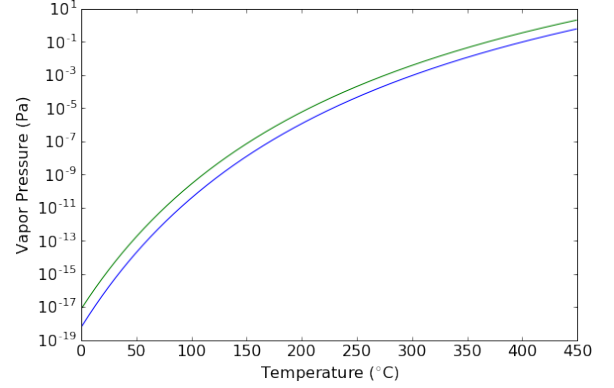


Figure 1: Vapor Pressure (Pa) of Yb (Blue) and Mg (Green) as a function of Temperature (°C). Data is extracted from equations given in [1].

3.2 Atomic Beam

The atomic beam exits the oven aperture and traverses through the SAM vacuum system. This vacuum system consists of a straight path from the oven aperture to the cryostat. The diameter of the vacuum chamber is $\sim 2.3''$, allowing for a maximum atomic beam diameter of that size. Any atoms that hit the surface of the vacuum chamber will instantly crystallize. I approximate the angle of divergence for the atomic beam through the assumption that $\theta_{max} = \tan^{-1} \frac{2r}{l}$. According to theory[2], the intensity of the atomic beam resembles a cosine distribution. I approximate the spatial distribution of the atomic beam as a flat distribution.

3.3 Laser Beam

The laser beam used to probe the atomic beam is supplied by a pump laser outputting into a tunable TiSapphire laser cavity and a frequency doubling cavity. The resulting laser can be measured with 10^{-4} nm precision. The spatial distribution of photons is Gaussian in shape, and can be measured using a beam profiler. The spectral distribution is a gaussian shape about a chosen central λ (10^{-4} nm precision). The shape is relatively narrow when compared to the FWHM of the atom's spectral lineshape. The number of photons per unit time per unit area as a function of laser frequency ν , radial distance from the beam's center r , distance along the central beam axis z and time t , can be written:

$$\Phi(\nu, r, z, t) = \frac{2P_0}{\pi w(z)^2 h\nu_0} \text{Exp}\left[\frac{-2r^2}{w(z)^2}\right] \frac{2\sqrt{\log(2)}/\pi}{FWHM} \text{Exp}\left[-4\log 2 \frac{(\nu - \nu_0)^2}{FWHM^2}\right], \quad (3)$$

$$w(z) = w_0 \sqrt{1 + \psi_0^2 \left(\frac{z - z_0}{w_0}\right)^2} \quad (4)$$

where P_0 is the peak laser power, $w(z)$ is the beam radius as a function of distance along the central beam axis, ν_0 is the central laser frequency, $FWHM$ is the full width at half maximum of the laser's spectral distribution, w_0 is the laser beam width, $\psi_0 = \lambda/(\pi w_0)$ and z_0 is the position of the beam waist along the central beam axis.

4 Atomic Beam Fluorescence Measurements

Atomic beam flux measurements are performed using the Single Atom Microscope setup, the BLUREI laser in Spinlab, and various optics, optomechanics and electronic devices. This experiment probes the strong Yb $^1P_1 - > ^1S_0$ transition through laser excitation of the atomic beam. The spontaneous emission of the atoms is measured using an avalanche photodetector set up at 90° to the excitation laser. Using arguments for detector efficiency, geometry and properties of the atomic and laser beams, a yb number density in vacuum can be extracted from these measurements.

The schematic of this setup is shown in figure 2. The signal from the photodetector is amplified and extracted using an optical chopper paired with a lock-in amplifier.

The operating procedures for atomic beam fluorescence measurements can be found at I:/projects/spinlab/SADiCS/Setup_NSCL/Instructions_Procedures/170621_ABF_Procedures.docx.

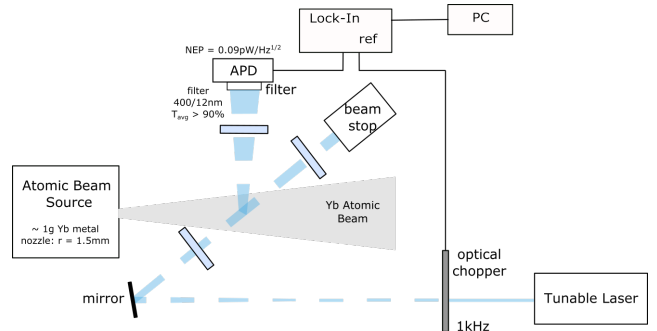


Figure 2: Schematic of the setup for ABF measurements.

4.1 Experimental considerations

Many aspects of the experiment must be studied and documented in order to properly determine the Yb number density. It is important to understand the atomic structure of Yb as well as the properties of the vacuum system, yb oven and excitation laser. Ideally, we would know the exact location, size and spatial distribution of the laser and atomic beams. We would also know the geometry of the setup exactly and have completely eliminated all light entering the APD aside from the atoms' fluorescence. Since we can't know these things exactly, I will explain how I've tried to measure these things precisely.

In order to measure the laser power to a high precision, I measure the laser power immediately before it enters the vacuum system. This should be done as close to the time of the measurement as possible, since the power could drift over time. It is important to have all elements of the experiment in place and running, such as the optical chopper, at the time of the power measurements as these elements reduce the laser power. In order to monitor the stability of this laser power during the experiment, a beam splitter is used to sample a portion of the laser beam and measure its power throughout the experiment.

This fraction of the laser's total power is recorded and can be used to adjust the power claimed to be entering the vacuum accordingly. I do not account for the power loss from the windows at the 6-way cross. I also measure the power at various locations along the beam path and at various times as a means to understand how the beam changes over distances and after being directed by different optical elements.

I measure the shape and intensity distribution of the laser using a beamprofiler, BP209. Currently I take a measurement before and after all measurements are done, assuming that these two beam profiles can be averaged. I do not expect the shape and intensity of the beam to change enough to throw off the results of the experiment, but this could be studied further. I also measure the beam profile at multiple locations along the beam path to study how this profile changes.

In order to measure a small fluorescence signal above what is sometimes a relatively large noise signal, an optical chopper is used. The optical chopper chops the laser beam at a chosen frequency and sends a reference signal to the lock-in amplifier. The lock-in amplifier locks only to signals that are also oscillating at the same frequency. In this case the fluorescence signal measured at the APD should be the only signal oscillating at that chosen frequency. The optical chopper must chop at a frequency much faster than the change in measured signal relative to the average signal in order to prevent the lock-in from having difficulties locking to a signal.

In order to pick out a sometimes small fluorescence signal, the background light must be mitigated. To lessen the scattering of light, the inside of the 6-way cross is covered in black foil. The APD is attached to a bandpass filter (FF01-400/12-25) which is directly connected to a lens tube. This lens tube comes as close as possible to the vacuum system to prevent lights from the room from entering the APD. The fluorescence emitted from the excited atoms is very nearly isotropic, so the only light I expect to enter the detector comes from fluorescence of Yb atoms.

The geometry of the setup must be carefully noted in order to accurately determine the solid angle of fluorescence measured by the detector. I calculate the light collection efficiency of the detector using:

$$\frac{\Omega}{4\pi} = \frac{A_{det}}{4\pi d_{det}^2}, A_{det} = \pi r_{det}^2, \quad (5)$$

where A_{det} is the area of the active area of the detector, r_{det} is the radius of the active area of the avalanche photodiode and d_{det} is the distance to the detector from a point within the fiducial volume. This light collection efficiency is valid when $\sqrt{A_{det}} \ll d_{det}$.

Isotope shifts and hyperfine shifts complicate the spectrum of Yb for this transition. The laser must be scanned over a range of frequencies in order to excite all yb atoms of various isotopes and total angular momentum values. The current parameters I use for frequency scans(fine terascan) are:

Scan center:797.8228nm
 Scan width:3GHz
 Scan rate:10MHz/s.

This range is chosen in order to include all of the frequency splittings for this transition, but it is a bit overkill. A new scan range can be determined by calculating the range more precisely or by looking in this paper [3]. I picked this rate in order to get a very detailed scan($\sim 2 \times 10^{-5} nm/s$), this may be adjusted, but I haven't thought in depth

about the best scan rate. This laser frequency cannot be electronically readout on a windows 7 computer, but the resonator slow voltage output of the laser can be sent to the DAQ card used for the measurement. A frequency to voltage calibration can be done over the range of frequencies we are interested in. This calibration will be different for other ranges of frequencies. A time varying voltage offset must be determined for each frequency scan, and can be extracted from recorded data. I currently do this by hand.

In order to create a full calibration of the atomic oven, ABF measurements must be taken at a variety of different atomic oven temperatures, starting at 450°C and ending at a temperature where there are no more atoms flowing in the system. The experimenter should wait until the temperature of the oven has stabilized before taking data at that temperature. Eventually the measurements are no longer possible as the number of atoms in the system is not large enough to create a fluorescence signal strong enough to be seen above the noise floor. Currently, a signal cannot be detected below $\sim 275^{\circ}\text{C}$. The lower temperature limit can vary depending on the pressure of the vacuum system [figure 1].

4.2 Data Collection

The experiment is run using the jabf.vi found in I:/projects/spinlab/SADiCS/Programs/LabVIEW VIs/ABF. Most of the important values in the experiment can be recorded in this program: time, yb oven temperature, lock-in signal, power meter voltage, resonator slow voltage and the standard deviations of these values. The pressure reading in the vacuum system would be useful to add to the vi in order to approximate at which temperature the atoms are no longer vaporized as well as determine if a signal is typically recorded at a given temperature and pressure. This vi will automatically output the necessary data without pushing extra buttons on the vi, but it must run throughout the entirety of a frequency scan if all data is to be gathered.

Values such as the conversion scale of the Thorlabs power meter and the gain of the APD must be noted by hand. Gentec power meters are done with the Gentec software and beam profile measurements are done with the Thorlabs software.

In order to create a frequency to resonator slow voltage calibration, the resSlowVolt_freq_calib.vi in I:/projects/spinlab/vis_Labview/Laser VIs can be used on the laser computer. This should be ran during a scan over the frequency range of interest. The program outputs time, wavelength, frequency and resonator slow voltage. There is already a calibration for the current range of frequencies, but in the future a scan over a different range of frequencies may be desired.

4.3 Data Analysis

The data analysis program, abf_dataAnalysis.m, is written in Matlab and can be found at I:/projects/spinlab/SADiCS/Programs/MATLAB. This program determines the flux of Yb atoms at the 6-way cross given the measured data:

$$Flux = \frac{F \cdot v_{rms}}{V_{fid} \cdot R \cdot \frac{\Omega}{4\pi}}, \quad (6)$$

where F is the photon detection rate, v_{rms} is the rms velocity, V_{fid} is the fiducial volume, R is the excitation rate per atom and $\frac{\Omega}{4\pi}$ is the light collection efficiency of the detector.

This analysis program will prompt for an input data file produced by the jabf vi, which will correspond to a measurement at a certain temperature. Each row of data in

the data file contains the recorded values at a certain time. Since this data was gathered during a laser scan, we can expect that as we progress through the data the frequency will be changing. The starting and stopping resonator slow voltages of the scan are currently hard coded into the program, in order to pick the data from the scan. These values were found by hand.

The program also prompts for a laser power data file of .csv type. This file should be saved when measuring the power directly before starting a scanning measurement. Once the laser power data is selected, the program averages the power readings in the data file and determines the peak laser power. The program then uses the voltage readings from the Thorlabs power meter to monitor the power stability and make any adjustments when power fluctuations occur.

The beam profile data is currently only used to find the major and minor beam radii. I take two beam profile measurements before and after the experiment and average the measured radii. The laser beam is approximated as a circle with a radius that is the average of the two radii of the ellipse. The radius is hard coded into the program. The intensity distribution is approximated as a uniform distribution as opposed to a Gaussian distribution. Under the approximation, the laser beam photon flux becomes:

$$\Phi = \frac{2P_0}{\pi w^2 h \nu}, \quad (7)$$

where P_0 is the peak laser power, w is the beam radius, h is planck's constant and ν is the laser frequency.

The signal from the lock-in amplifier is read out as an x and y signal. These can be transformed to a total amplified signal:

$$R = \sqrt{x^2 + y^2} \quad (8)$$

This amplified signal can be used to extract the number of photons hitting the avalanche photodetector:

$$N = \frac{R}{\frac{\mathcal{R}(\lambda)}{50} \cdot M \cdot G \cdot h \nu}, \quad (9)$$

where $\mathcal{R}(\lambda)$ is the detector responsivity, which can be determined by figure 3, M is the gain of the detector (5-50) and G is the amplifier's transimpedance (500kV/A).

The velocity of the atoms in the vacuum system can be described by a Maxwell-Boltzmann distribution:

$$f(v) = \sqrt{\left(\frac{m}{2\pi kT}\right)^3} 4\pi v^2 e^{\frac{-mv^2}{2kT}}, \quad (10)$$

where m is the atom's mass, k is Boltzmann's constant, T is the temperature of the atom & oven and v is the velocity of the atom. We can expect that the spectral line shape will be Doppler broadened, but only due to the portion of the velocity in the direction of the laser beam.

I calculate the atomic cross section using:

$$\sigma_i = \pi r_e c f \mathcal{L}(\nu), \mathcal{L}(\nu) = \frac{\frac{\Gamma}{2\pi}}{(\nu - \nu_0)^2 + \frac{\Gamma^2}{4}}, \quad (11)$$

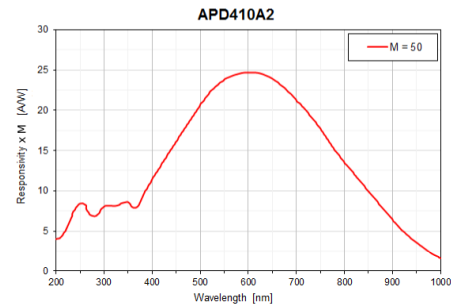


Figure 3: APD410A2 Responsivity*M (A/W) as a function of wavelength. This plot is from the manufacturer, Thorlabs.

where r_e is the classical electron radius, c is the speed of light, f is the oscillator strength for this transition and $\mathcal{L}(\nu)$ is the Lorentzian line shape function at ν for this transition.

The fiducial volume for this experiment is the volume of intersection between the laser beam and the atomic beam. In this volume, the atoms can be excited and emit light into the detector, so it is important to understand which portion of the total atomic beam volume is excited. I approximate the fiducial volume for each possible atomic velocity as the following:

$$V_{fid}(v) = \frac{\pi w^2}{n f(v) \cdot \sum_i \sigma_i P_i}, \quad (12)$$

where $f(v)$ is the Maxwell Boltzmann distribution at a velocity v , σ_i is the cross section for isotope i at a given frequency and P_i is the fraction of isotope i in natural Yb.

The number of atoms in the fiducial volume can be calculated by:

$$N_{fid} = \frac{N}{R \cdot \frac{\Omega}{4\pi}}, \quad (13)$$

where N is the number of photons hitting the APD and R is the net excitation rate.

The atomic flux can then be deduced:

$$Flux = N_{fid} \cdot \sum_i \frac{v_i}{V_{fid}(v_i)} \quad (14)$$

4.4 Measurements to date

Date	Experiment Summary	Notes
06/15/2017	Laser scan center: 797.8228nm, width: 3GHz, rate: 10MHz/s. $\sim 305^\circ C - \sim 275^\circ C$.	Noise floor found at $\sim 275^\circ C$. Check that standard deviations were recorded.
05/15/2017	Laser scan center: 797.8228nm, width: 3GHz, rate: 10MHz/s. $\sim 345^\circ C - \sim 295^\circ C$	
12/05/2016	Excitation at single frequency (797.8224nm), black foil in chamber. $\sim 345^\circ C - \sim 225^\circ C$.	Lower temp limit found at $\sim 245^\circ C$.
10/06/2016	Excitation at single frequency (797.8228nm), $\sim 328^\circ C - \sim 70^\circ C$ (well below lower temp limit)	Resonance found by hand, all measurements performed at one lock-in sensitivity, laser beam diameters recorded by hand
07/26/2016	Excitation at single frequency (555.8023nm) to excite $^3P_1 - ^1S_0$ transition (GRUVY, BLUREI not working), $\sim 50mW$ of light, fiber coupled, lockin sensitivity not adjusted at proper intervals. $\sim 445^\circ C - \sim 103^\circ C$ (well below lower temp limit).	Data recorded by hand, temperature was not stable during measurements, no beam profile measurements

5 Atomic Beam Flux Simulation

The atomic beam flux simulation calculates the flux at a chosen location along the atomic beam path,

$$Flux = \frac{Q}{\pi R^2}, \quad (15)$$

where Q is given in equation 1 and R is the radius of the atomic beam at the chosen location. For our purposes, it is most useful to simulate the flux at the position where ABF measurements occur, the 6-way cross.

The simulation is most useful if it predicts the signal measured by the APD during an atomic beam flux measurement, but this has yet to be implemented. The predicted signal can be used for quick comparisons during measurements. It is also useful for simulating a desired change to the experiment.

To expand upon the simulation, the excitation rate for yb atoms of various isotopes and total angular momentum values must be well understood theoretically. The frequency spacings and isotopic abundances listed above can be used to predict the location of a resonant frequency. The spectral shapes can be determined by considering the convolution of the natural Lorentzian lineshapes with Doppler broadened lineshapes. I am unsure if other broadening factors play a role in the final lineshape. The excitation rate of a given isotope can be calculated by:

$$R_i = \int_0^\infty \sigma_i(\nu) \phi(\nu) d\nu = \frac{P_0}{h\nu_0} \frac{2}{\pi w^2} \text{Exp}\left[-\frac{2r^2}{w^2}\right] \pi r_e c f \int_0^\infty \mathcal{L}(\nu) \mathcal{G}(\nu), \quad (16)$$

where ν_0 is the central frequency of the laser. When the FWHM of the spectral distribution of the atom's cross section is much greater than the FWHM of the laser's spectral distribution, the excitation rate reduces to:

$$R_i = \frac{2P_0}{\pi w^2 h\nu_0} \text{Exp}\left[-\frac{2r^2}{w^2}\right] \pi r_e c f \mathcal{L}(\nu_0), \quad (17)$$

6 Uncertainty

In the table below, uncertainty of experimental quantities are stated.

Experimental factor	Uncertainty	Considerations
Laser Power		Accuracy and precision of power meter, loss of light through window
Wavelength		Accuracy and precision of wave meter and laser, uncertainty in resonator slow voltage fit
Detector Efficiency		Accuracy and precision of manufacturer's conversion efficiency
Voltage readings from lock-in		
Light collection efficiency		Accuracy and precision of approximation for efficiency, assumption that fluorescence is isotropic, loss of light through window
Fiducial Volume		Assumption of divergence angle of atomic beam
Origin of photons		Assumption that fluorescence is the only light hitting the detector
Velocity of atoms		Accuracy and precision of temperature sensor, assumption that all atoms at temperature of temperature sensor
Laser beam spatial distribution		Assumption that spatial distribution is uniform throughout circular area
Laser beam spectral distribution		Assumption that distribution is a delta function at central frequency
Atomic beam spatial distribution		Assumption that distribution is uniform
Atom's lineshape for transition		Accuracy and precision of measured lineshape

References

- [1] C. B. Alcock. Vapor pressure of the metallic elements, 2000.
- [2] Norman F. Ramsey. *Molecular Beams*. Oxford University Press, 1956.
- [3] Dipankar Das *et al.* *Phys. Rev. A*, **72**, 032506, 2005.